Nuclear Instruments and Methods in Physics Research A 596 (2008) 396–401

Contents lists available at ScienceDirect

Nuclear Instruments and Methods in Physics Research A

journal homepage: www.elsevier.com/locate/nima

After-pulsing and cross-talk in multi-pixel photon counters

Y. Du [a], F. Retière [b,*]

[a] Department of Physics and Astronomy, University of British Columbia, 6224 Agricultural Road, Vancouver, BC, Canada V6T 1Z1
[b] TRIUMF, Science, 4004 Wesbrook Mall, Vancouver, BC, Canada V6T 2A3

ARTICLE INFO

Article history:
Received 17 January 2008
Received in revised form
18 July 2008
Accepted 12 August 2008
Available online 28 August 2008

Keywords:
Photo-detector
Scintillator
Avalanche photodiode
GPD
MPPC

ABSTRACT

Multi-pixel photon counters (MPPC) are pixelated Geiger-mode photon manufactured by Hamamatsu photonics. They will be used for reading out all the scintillator elements within the near detector of the T2K experiment. Their performances photo-detection efficiency, dark noise and gain, and their insensitivity to magnetic field fulfill the ND280 requirements. On the other hand, two known issues, cross-talk and after-pulsing may adversely impact the detector response. In this paper, cross-talk and after-pulsing are precisely measured by recording waveforms and identifying all the avalanche pulses. At an over-voltage of 2 V, an avalanche generates on an average 0.5 additional avalanches due to after-pulsing, whereas it generates 0.13 at 1 V over-voltage. After-pulses follow two independent time constants of 15 and 82 ns. The cross-talk probability is a factor of 3 smaller than the after-puling probability. Simulating the MPPC response, we find that after-pulsing and cross-talk do not degrade the detector performance significantly within the expected operating conditions of the T2K near detector.

1. Introduction

1.1. The T2K near detector experiment

The T2K near detector (ND280) is designed to detect a fraction of the neutrinos produced by the J-PARC accelerator complex [1,2]. The building block of most ND280 detector elements (on axis detector, fine grain detector, electromagnetic calorimeter, pi0 detector, and side muon range detector) is a Kuraray Y11 wavelength shifting (WLS) fiber threaded through a plastic scintillator bar and readout on one or both ends by a photosensor. Most of the photosensors are enclosed within a 0.2 T magnet, which rules out using simple photo-tubes. The recently developed pixelated Geiger-mode avalanche photon detectors (PPD) have been chosen in place of photo-tubes or avalanche photodiodes. Indeed, they provide a much larger gain than standard avalanche photodiodes, while matching or surpassing the photo-tube photo-detection efficiency, and being insensitive to magnetic field. While PPDs appear to be a perfect solution for experiments such as T2K ND280, being newly developed devices, they have not been characterized in depth. The aim of this paper is to investigate quantitatively two possible drawbacks: after-pulsing and cross-talk, in order to determine to which extent they affect the detector performance.

The most important detector performance that must be achieved is a detection efficiency of 100% for minimum ionizing particles (MIPs). Accounting for channel-to-channel variation and the low-energy tail of the energy loss, this translates to requiring the average number of photo-electrons produced by a MIP to be at least 15. The light coming out of the WLS fiber is not emitted instantaneously but is fully collected in about 50 ns, mostly due to the WLS fiber decay time constant of 9 ns. The T2K ND280 electronics hence has to integrate the PPD current for at least 50 ns. In practice, the integration time will follow the beam spill structure to be about 500 ns depending on the accelerator operation mode. Most ND280 elements will use such electronics based on the TRIP-t ASIC that also provides a discriminator output per channel [3]. The discriminator triggers when the integrated charge exceeds a programmable threshold, providing a signal that is subsequently time stamped by a field programmable gate array. The fine grain detector electronics is based on a waveform digitization scheme sampling at 50 MHz for 10 μs [4]. In order to achieve the required timing resolution, the PPD pulses are stretched by a RC-CR2 preamplifier shaper with a 120 ns peaking time. Both electronics are expected to achieve the required timing resolution of 3 ns or better. The energy resolution requirement is modest. The energy information will be used mostly to identify muons from protons. The requirement for the PPD is that effects such as dark noise, cross-talk or after-pulsing do not affect the energy resolution and the timing resolution, which should both be driven by the statistics of the number of photo-electrons.

* Corresponding author. Tel.: +1 604 222 7572; fax: +1 604 222 1074.
E-mail address: fretiere@triumf.ca (F. Retière).

0168-9002/$ - see front matter Crown Copyright © 2008 Published by Elsevier B.V. All rights reserved.
doi:10.1016/j.nima.2008.08.130

1.2. Pixelated Geiger-mode avalanche photon detectors

PPD, also called silicon photo-mutipliers (SiPM) are becoming a mature technology, both for particle physics and medical imaging [5–7]. A PPD is an array of 100 to several 1000 s photodiodes arranged into square pixels operating in Geiger-mode with a current limiting resistor. Free charge carriers drifting through the depleted region are able to free additional carriers when the reverse bias voltage across the junction goes above a critical breakdown voltage (VBD). An avalanche develops as described in Ref. [8] until the current flowing through the resistor (R) in series with the diode brings the voltage across the junction to VBD. The maximum current flowing through the diode is $I_{\max} = \Delta V/R$, ΔV being the over-voltage, i.e. the difference between the reverse bias and VBD. The total charge per avalanche is governed by the diode capacitance (C): $Q = C\Delta V$. The output current of the PPD is the sum of all the diode currents. The number of photons hitting the device is measured by counting the number of pixel avalanches. The photon detection efficiency is the probability that a photon triggers an avalanche when hitting a PPD. The response is linear if (i) the number of pixel avalanches detected is small ($<15\%$) compared to the total number of pixels, and (ii) the light is uniformly distributed across the surface.

An avalanche in 1 pixel at a given time can trigger additional avalanches either in neighboring pixels or in the same pixel at a later time. The former phenomenon is called cross-talk whereas the latter is called after-pulsing. Cross-talk is believed to be caused by photons produced in an avalanche, which knock off electrons in a neighbor pixel and trigger an additional avalanche [9]. It has been recently shown that the trajectories of the cross-talk inducing photons may not be straight lines but instead go through reflections within the substrate [10]. Either way, the photon propagation time is very short, hence the original and neighbor avalanches occur essentially at the same time.

On the other hand, an after-pulsing avalanche occurs after the original avalanche. It is believed to be triggered by the release of a charge carrier that has been produced in the original avalanche and trapped on an impurity [11,12]. It is also possible that the photons produced in the original avalanche generate after-pulses if instead of knocking of an electron in the depletion region of a neighbor pixel, they do so within the silicon substrate. One of the charge carriers hence produced may eventually find its way back to the pixel and trigger a second avalanche. This phenomenon was observed in Ref. [13] but the carriers were found to diffuse back into the depletion region in <1 ns, which would be invisible to PPDs. However, the PPD doping profile may allow for much longer carrier diffusion time within the substrate.

1.3. Multi-pixel photon counters (MPPCs)

MPPCs are PPDs designed and manufactured by Hamamatsu photonics [14,15]. They have been extensively tested in the context of the ND280 detector within the T2K experiment [4,5,16], together with similar devices [17]. A total number of about 50,000 MPPCs will be used in the T2K experiment. Their performances fulfill the detector requirements. A large gain ($>500{,}000$), and large ($>15\%$) photo-detection efficiency can be achieved while maintaining the dark noise rate below 1 MHz.

The MPPCs that were tested in this paper have 400 pixels ($50\times 50\,\mu m^2$) covering a total area of 1 by 1 mm^2. A 100 kΩ resistor is used for quenching the avalanche. The total capacitance of the device is 35 pF, which translates into 87.5 fF per pixel ignoring parasitic capacitances. With a 1 V over-voltage, the gain, i.e. the number of electrons produced by 1 photo-electron in 1 pixel is about 550,000.

2. Measuring cross-talk and after-pulsing

2.1. Test setup

The MPPC was housed in a light tight tube. The data were taken at a temperature of 25 °C. A Keithley 6485 picoammeter was used to bias the MPPC between 69.4 and 70.6 V through a 100 kΩ resistor. The MPPC pulse was readout by decoupling the bias line with a 1 nF capacitor. A custom amplifier was used to achieve a gain of 10 before feeding the signal into a CAEN V1729 waveform digitizer sampling for 2.5 μs at 1 GHz. The trigger was generated by further amplifying the signal using a CAEN N978 amplifier and a discriminator, with the threshold set to 0.1–0.2 avalanche equivalent signal, depending on the MPPC bias voltage.

2.2. Waveform analysis: pulse finding

Two events with multiple pulses are shown in Fig. 1 to illustrate the pulse finder's ability. Most events have only one pulse at 270 ns, which is where the trigger happens to be. A pulse finder analysis was performed on the waveforms in order to measure the time and amplitude of the avalanches occurring within the acquisition window. The pulses were found in two steps. First, all the pulses with a signal-to-noise ratio over 5 were identified unless they were too close to an earlier pulse, because the first pass algorithm required the signal to return to the baseline before accepting a subsequent pulse. The waveforms were then fitted by a superposition of single avalanche response functions (SARF). The SARFs were extracted directly from the data by calculating the average waveforms for events that have only 1 avalanche within a 150 ns wide integration window around the trigger pulse. An analytical function fitting the SARFs perfectly could not be found and standard spline interpolation techniques would smooth out the SARF too much. A linear interpolation of the SARFs was used instead, which yield to about 1 ns resolution in the reconstruction of the pulse arrival time.

The correlation between the pulse amplitude and trigger time introduced by the leading edge discriminator was corrected for before calculating the average waveform. A χ^2 was computed to assess the quality of the fit. The number of degrees of freedom (dof), i.e. the fit range, was set to 50 unless two or more pulses partially overlapped, in which case the fit range was extended to encompass all the pulses. If the χ^2 per dof (χ^2/dof) was found to be more than 5, an additional pulse was added and the fit was re-run. Pulses were added until the χ^2/dof fell below 2 or until 5 additional pulses were added. This method was reliable to find pulses close to each other, even when they almost fully overlap because the shape of the waveform provides a strong constraint.

2.3. Extracting cross-talk

The time and amplitude of the pulses found in a 500 ns window following the trigger are shown in Fig. 2. The time is defined with respect to the trigger pulse time. The amplitude is the scale applied to the SARFs to reproduce the data, so it is automatically proportional to the signal given by the avalanche at nominal gain. The trigger pulses can be seen at time zero as 3 narrow bands at 1, 2, and 3 avalanches. Cross-talk can be extracted directly from the frequency distribution of trigger pulse amplitude obtained by the projection of these bands onto the y-axis. Cross-talk is calculated as the probability that 1 pixel triggers at least 1 avalanche in a neighbor pixel: $1-N_1/N_{\text{total}}$ with N_1 being the number of 1 avalanche pulses and N_{total} the total number of trigger pulses. The trigger sample is selected by using a 1 ns time window, which ensures that the contribution of after-pulsing is

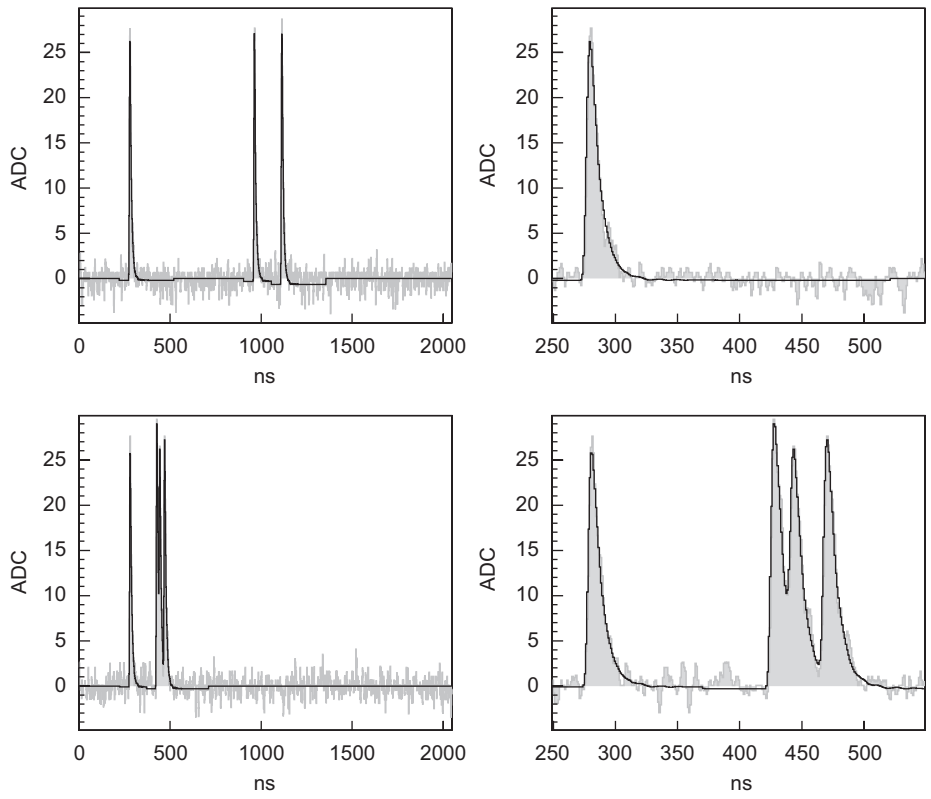

Fig. 1. Two events taken at 70 V bias and 25 °C (1.3 V overvoltage). The right-hand panels are zooms around the trigger pulse. The filled grey histogram is the data and the black curve is the fit.

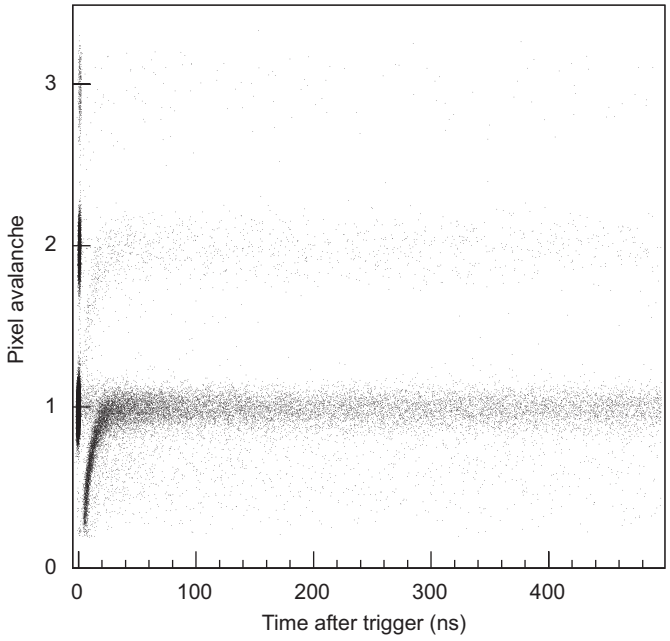

Fig. 2. Amplitude and time distribution of all the pulses found by the pulse finder at 70 V bias and 25 °C (1.3 V over-voltage).

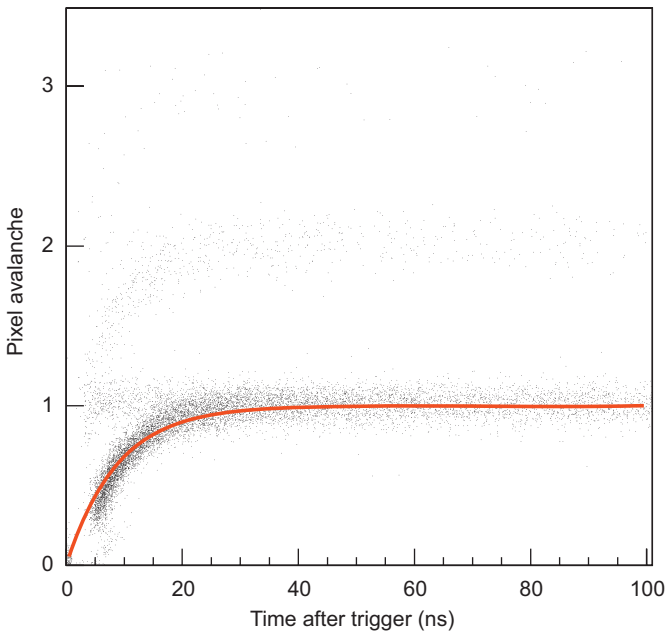

Fig. 3. Amplitude and time distribution of the first pulse following the trigger pulse at 70 V and 25 °C (1.3 V over-voltage). The solid red curve shows the expected single pixel recovery.

negligible. Indeed, within 1 ns immediately following an avalanche, the pixel over-voltage is close to zero. Hence, if a charge carrier happens to enter or be released within the depleted region 1 ns or less after the first avalanche, it will not generate an avalanche.

2.4. Pixel recovery

The over-voltage recovery is clearly visible in Fig. 2 as a band below 1 avalanche between 0 and 40 ns after the trigger. Fig. 3 presents a clearer view of recovery in a 100 ns window following

the trigger. The recovery behavior is well reproduced by the expected function $1-e^{-t/\tau}$, with $\tau = 100\,k\Omega \times 8.75\,fF = 8.75\,ns$.

2.5. Measuring after-pulsing

Each avalanche may result in trapped charge carriers. However, as discussed earlier, it is possible that some of the after-pulses have nothing to do with trapped carriers but originate instead from charge carriers created by photons in the substrate, in the same fashion as cross-talk. In order to avoid making unnecessary assumptions, we will quantify after-pulsing as the average number of delayed carriers triggering an additional avalanche per original avalanche. This nomenclature has the advantage of accounting for the fact that a carrier released while the voltage is not fully recovered will have a smaller probability of triggering an avalanche than at the nominal operating voltage.

We build the timing distribution of the first pulse following the trigger pulse, because the probability distribution of the first pulse arrival time is fairly simple to express mathematically, which is not the case when multiple after-pulses created by avalanches following the trigger pulse have to be considered. We select trigger pulses with only one simultaneous avalanche, hence discarding the ones with cross-talk. We also ensure that no avalanche happened within the 270 ns before the trigger pulse in order to avoid selecting avalanches that may themselves be after-pulses. The amplitude and time distribution of the first pulse following the trigger pulse is shown in Fig. 3. This figure is very similar to the one shown in Ref. [18]. Three bands for 1, 2, and 3 pixel avalanches are clearly visible when the pulses occur later than 40 ns after the trigger. Cross-talk is responsible for the 2 and 3 pixel avalanche bands. The bands split into two for the pulses within 40 ns after the trigger: one constant and the other following the pixel recovery time constant as discussed earlier. The constant band is unaffected by the pixel recovery, hence must originate from a different pixel than the trigger pulse. It is presumably due to thermally generated dark pulses. On the other hand, after-pulses occurring earlier than 40 ns after the trigger have reduced gains because the over-voltage is not recovered to its original level.

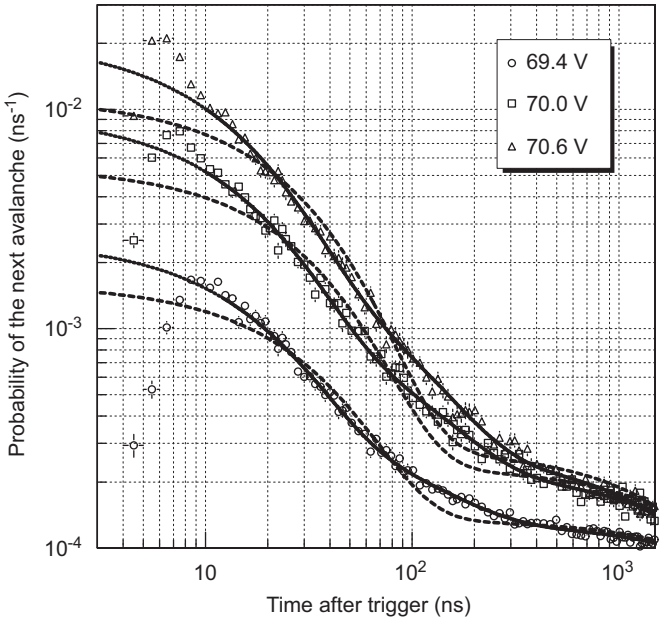

Fig. 4. Timing distribution of the first pulse following the trigger. The dotted lines are fits with a single after-pulsing time constant, while the solid lines included two time constants. The dashed lines show the two exponential function behaviors beyond the fit range.

Fig. 4 shows the time distribution of the first pulse following the trigger for three different bias voltages. The first pulse following the trigger pulse comes either from after-pulsing or from dark noise. The probability of the first pulse occurring in the time interval t and t+dt, is an after-pulse is

$$P_{AP}(t) = \sum_{i=1}^{\infty} \frac{\lambda^i}{i!} e^{-\lambda} \frac{i}{\tau} e^{-t\cdot i/\tau}$$

with λ being the average number of delayed carriers triggering an avalanche per original avalanche, τ, the carrier release or diffusion time constant. The probability for a thermally generated dark pulse is

$$P_{DN}(t) = Re^{-Rt}$$

with R being the dark noise rate. The sum over the Poisson probability accounts for the possibility of having more than one delayed carrier created per avalanche, which was not taken into account in Ref. [4]. When combining after-pulses and thermally generated dark pulses, the probability must be mutually exclusive, i.e. a dark (after) pulse occurring at t with no after (dark) pulse occurring between 0 and t, which leads to the probability

$$P(t) = \int_0^t [1 - P_{AP}(x)]\,dx P_{DN}(t) + \int_0^t [1 - P_{DN}(x)] \times dx P_{AP}(t).$$

The dotted curve in Fig. 4 shows a fit using this function. The quality of the fit is poor, so a second after-pulse time constant has to be introduced to obtain a good fit. The fit is limited to time later than 10 ns because the pulse finder is not very accurate for finding pulses with significantly reduced gains, which typically occur within 10 ns after the trigger. While the pulse finding efficiency remains fair (except for low bias voltage), the fit parameters (time and amplitude) become less accurate, especially the pulse time, which tends to be shifted later due to an artifact in the pulse finder algorithm.

3. Parameterization of cross-talk and after-pulsing as a function of over-voltage

The parameters extracted from the fit using the 2 time constant after-pulsing models are summarized in Fig. 5, as functions of over-voltage. The VBD was found to be 68.7 V by extrapolating the gain down to zero. The after-pulsing parameter shown in this figure is $1-e^{-\lambda}$, the probability that an avalanche is followed by at least one after-pulsing avalanche. The errors are both statistical and systematic. The statistical errors dominate at low over-voltage whereas systematic ones dominate at above 1 V. The main source of systematic error comes from the lack of efficiency for finding the pulses in the 0–10 ns time interval. Indeed the probability distribution used in the fit assumes that the first pulse is always found. However, if it occurs too early to be detected, the second pulse will be substituted as the first pulse and distort the experimental time distribution. We performed simulations to estimate this effect. Assuming that all the pulses occurring 10 ns or less after the trigger pulse are missed, we found that the dark noise rate, the number of after-pulses per avalanche, and the long after-pulse time constant were overestimated by as much as 40%, 15%, and 15%, respectively, when those parameters are large, i.e. corresponding to an over-voltage of 1.9 V. On the other hand, the short time constant appears to be underestimated by as much as 15%. This effect was found to be small for the parameters corresponding to over-voltages <1.3 V. The error on the over-voltage is primarily due to day-to-day temperature variation.

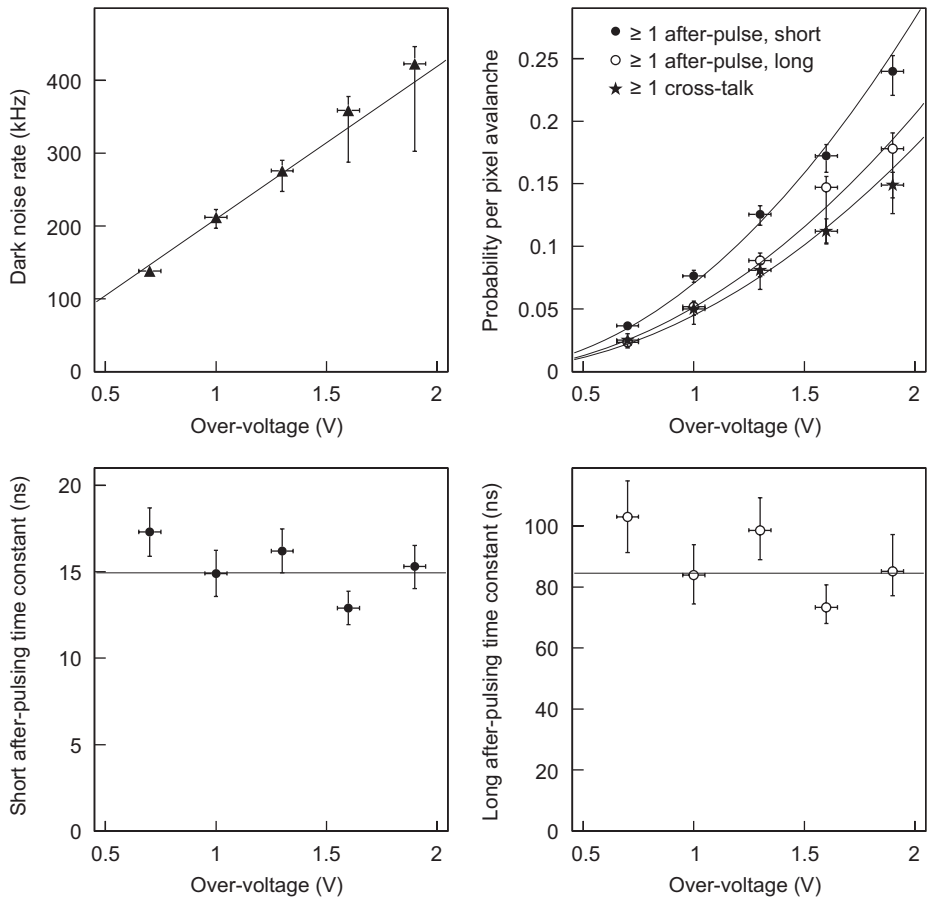

Fig. 5. Parameters extracted from the fits to the distribution of the arrival time of the first hit following the trigger.

The data shown in Fig. 5 were fitted to extract trends as a function of over-voltage. The dark noise rate rises linearly with over-voltage at a rate of 212 ± 9 kHz/V. The dark noise remains below 500 kHz even at 2 V over-voltage. The after-pulsing and cross-talk probabilities vary quadratically with over-voltage in the following fashion: $\text{Prob}(\text{AP}_{\text{short}}) = 0.073 \pm 0.003\,\text{V}^2$, $\text{Prob}(\text{AP}_{\text{long}}) = 0.054 \pm 0.003\,\text{V}^2$, and $\text{Prob}(\text{cross-talk}) = 0.044 \pm 0.002\,\text{V}^2$. Cross-talk is smaller than the sum of both short and long after-pulsing probabilities by roughly a factor of 3. At 1.9 V over-voltage (70.6 V at 25 °C), the average number of late carriers per avalanche is 0.5. At that level after-pulsing may become problematic. It is indeed not uncommon to see trains of avalanches produced by a single dark noise pulse. The average after-pulsing time constants are 15.0 ± 0.6 and 83.5 ± 3.9 ns. There appears to be a slight decrease of the time constants with over-voltage, which runs contrary to the expectation that the trap release time constant is independent of the bias voltage. As mentioned earlier, the robustness of the method has been verified by simulations and the necessary systematic errors have been included in the reported results. Nevertheless, the systematic errors on the long time constant are likely underestimated. Indeed calculating the long time constant with only the three lowest over-voltage points yields 92.7 ± 5.8 ns. The time constants measured for the MPPCs are consistent with the ones reported for single photon avalanche diode in Ref. [10], which suggests that after-pulsing can be interpreted solely as being due to trapping. In Ref. [10], a third time constant of about 1 μs has been found as well. However, our measurement method is not sensitive to it because thermally generated dark pulses dominate the timing distribution beyond 500 ns after the trigger.

4. Impact of after-pulsing and cross-talk on the T2K ND280 detector performance

In order to estimate the impact of cross-talk and after-pulsing, we have developed a Monte Carlo simulation code that allows turning each effect on and off. The simulations include an algorithm that tracks the operating voltage of every pixel dropping down the voltage to VBD as avalanches occur and recovering according to the 8.75 ns time constant. This algorithm is important because it introduces avalanches with reduced gains, which are clearly visible in the dark noise spectrum or for low light level (<20 avalanches). The simulations use a model for the photo-detection efficiency, consistent with preliminary data showing a linear increase up to 1.5 V over-voltage followed by an onset of saturation. Light is injected onto the MPPC following an exponential with a 9 ns decay constant emulating the emission of the WLS fiber. The time zero of the light pulse is chosen randomly within 540 ns, which corresponds to the beam bunch width. Signal amplitude and time are calculated by mocking up the electronics response. The signal amplitude is given by the integral of the avalanche charge within the 540 ns gate. Timing is obtained by generating a discriminator output when the integrated charge goes above a programmable threshold. The T2K fine grain detector uses different set of electronics, based on waveform digitization at 50 MHz. However, the conclusions drawn below for the gate and discriminator electronics remain qualitatively the same.

The number of pixels fired is chosen to be about 20 at 1 V over-voltage, according to beam test measurements for a minimum ionizing particle [4]. Cross-talk and after-pulsing increase the

average number of pixels avalanching from 20 to 23.2 and 29.3 to 49.3 at 1 and 2 V over-voltage, respectively. However, such increase does not help the photo-detection efficiency because the number of avalanches generated by dark noise also increases in the same fashion. At 1 V over-voltage, the energy resolution degrades from 21.3% without cross-talk and after-pulsing to 22.1% when they are turned on. At 2 V over-voltage, the energy resolution goes from 17.8% to 21.2%. Cross-talk and after-pulsing hence have a marginal impact on the energy resolution up to 2 V over-voltage. However, the energy resolution does not improve and eventually worsens beyond 1.5 V over-voltage as the photo-detection efficiency saturates, while cross-talk and after-pulsing keep on increasing rapidly. Nevertheless, in the T2K detectors, the MPPCs will be operated between 0.5 and 1.5 V over-voltage, which means that cross-talk and after-pulsing will not affect the energy resolution significantly.

The simulations also show that cross-talk and after-pulsing have very little impact on the timing resolution obtained with the TRIP-t electronics as long as the programmable threshold is selected carefully. Indeed, it is crucial to ensure that the discriminator does not trigger on noise, which is likely to happen if the threshold is set low and the light pulse occurs late within the integration window. When using the electronics with slow preamplifier shapers, effect of after-pulsing on the timing resolution can be successfully mitigated by fitting only the rise time of the pulse and not the full waveform. Overall, the simulations show that cross-talk and after-pulsing do have visible effects in the charge and timing distributions, and thus must be taken into account, but they do not affect the detector performances significantly.

5. Conclusions

We have measured after-pulsing probabilities and time constants for 400 pixel MPPCs at room temperature with good accuracy. At 2 V over-voltage, the average number of delayed carriers that can trigger and after-pulse is larger than 0.5. The cross-talk probability remains below 0.2 at 2 V over-voltage. While such large after-pulsing and to a lesser extent cross-talk probabilities appear to be a concern, simulations show that they do not affect the energy nor timing resolution significantly at the operating voltage that is expected to be used by the ND280 detectors.

In the future, it would be beneficial to redesign the MPPCs by increasing the quenching resistor from 100 to 500 kΩ or more effectively by changing the quenching circuit from a passive one to an active circuit. If avalanches were followed by a 50 ns voltage drop to the VBD, then after-pulsing would be reduced by more than a factor of 2.

The authors wish to thank the ND280 photosensor group for fruitful discussions, Thomas Lindner and Antonin Vacheret for providing many useful suggestions regarding the experiment and the manuscript, Thomas Lindner and Scott Oser for providing the simulation code, Roman Tacik for pioneering the use of single avalanche response functions, the TRIUMF DAQ group for setting up the waveform digitizer and Leonid Kurchaninov for providing the low noise amplifier and the TRIUMF pienu experiment for supporting Yubo Du's work.

References

[1] Y. Itow, et al., The JHF-Kamioka neutrino project, hep-ex/0106019, 2001.
[2] T2K ND280 Conceptual Design Report, T2K Internal Document; 〈http://www.nd280.org/info〉.
[3] A. Vacheret, M. Noy, M. Raymond, A. Weber, First results of the Trip-t based T2K front end electronics performance with GM-APDs, PoS(PD07)027.
[4] F. Retière, Using MPPCs for T2K fine grain detector, PoS(PD07)017.
[5] D. Renker, Nucl. Instr. and Meth. A 571 (2007) 1.
[6] P. Buzhan, et al., Nucl. Instr. and Meth. A 504 (2003) 48.
[7] P. Buzhan, et al., Nucl. Instr. and Meth.A 567 (2006) 78.
[8] R.J. McIntyre, IEEE Trans. Electron Devices ED-20 (1973) 637.
[9] W.J. Kindt, H.W. van Zeijl, S. Middelhoek, in: Proceedings of the 28th ESSDERC (1998) p. 192.
[10] I. Rech, A. Ingargiola, R. Spinelli, I. Labanca, S. Marangoni, M. Ghioni, IEEE Photonics Technol. Lett. 20 (2008) 330.
[11] S. Cova, A. Lacaita, G. Ripamonti, IEEE Electron Devices Lett. 12 (1991) 685.
[12] A.C. Giudice, M. Ghioni, S. Cova, F. Zappa, in: Proceedings of the 28th ESSDERC (2003) p. 347.
[13] A. Lacaita, S. Cova, M. Ghioni, F. Zappa, IEEE Electron Device Lett. (USA) 14 (1993) 360.
[14] K. Yamamoto, K. Yamamura, K. Sato, S. Kamakura, S. Ohsuka, T. Ota, H. Suzuki, IEEE NSS Conf. Rec. 2 (2007).
[15] K. Yamamoto, K. Yamamura, K. Sato, S. Kamakura, S. Ohsuka, T. Ota, H. Suzuki, Proc. Int. Workshop New Photon-Detectors (2007) (PoS(PD07)004).
[16] S. Gomi, T. Nakaya, M. Yokohama, H. Kawamuko, T. Nakadeira, T. Murakami, R&D of MPPC for T2K experiment, PoS(PD07)015.
[17] O. Mineev, et al., Nucl. Instr. and Meth. A 577 (2007) 540.
[18] H. Oide, H. Otono, S. Yamashita, T. Yoshiota, H. Hano, T. Suehiro, Study of afterpulsing of MPPC with waveform analysis, PoS(PD07)008.